

Received October 12, 2021, accepted October 27, 2021, date of publication October 29, 2021, date of current version November 9, 2021.

Digital Object Identifier 10.1109/ACCESS.2021.3124386

# A Multiple Pheromone Communication System for Swarm Intelligence

TIAN LIU<sup>ID1,2</sup>, XUELONG SUN<sup>ID1,2</sup>, CHENG HU<sup>ID1,2</sup>, (Member, IEEE),  
QINBING FU<sup>ID1,3</sup>, (Member, IEEE), AND SHIGANG YUE<sup>ID1,2</sup>, (Senior Member, IEEE)

<sup>1</sup>Computational Intelligence Laboratory/Lincoln Center for Autonomous Systems, School of Computer Science, University of Lincoln, Lincoln LN6 7TS, U.K.

<sup>2</sup>Machine Life and Intelligence Research Center, School of Mechanical and Electrical Engineering, Guangzhou University, Guangzhou 510006, China

<sup>3</sup>School of Mathematics and Information Science, Guangzhou University, Guangzhou 510006, China

Corresponding authors: Cheng Hu (c\_hu@gzhu.edu.cn) and Shigang Yue (syue@lincoln.ac.uk)

This work was supported in part by the European Union's Horizon 2020 Research and Innovation Program through the Marie Skłodowska-Curie Grant 691154 spatial-temporal information processing for collision detection in dynamic environments (STEP2DYNA) and Grant 778602 ultra-layered perception with brain-inspired information processing for vehicle collision avoidance (ULTRACEPT), in part by the National Natural Science Foundation of China under Grant 12031003, and in part by the China Postdoctoral Science Foundation Grant 2019M662837 and Grant 2020M682651.

**ABSTRACT** Pheromones are chemical substances essential for communication among social insects. In the application of swarm intelligence to real micro mobile robots, the deployment of a single virtual pheromone has emerged recently as a powerful real-time method for indirect communication. However, these studies usually exploit only one kind of pheromones in their task, neglecting the crucial fact that in the world of real insects, multiple pheromones play important roles in shaping stigmergic behaviors such as foraging or nest building. To explore the multiple pheromones mechanism which enable robots to solve complex collective tasks efficiently, we introduce an artificial multiple pheromone system (ColCOSΦ) to support swarm intelligence research by enabling multiple robots to deploy and react to multiple pheromones simultaneously. The proposed system ColCOSΦ uses optical signals to emulate different evaporating chemical substances i.e. pheromones. These emulated pheromones are represented by trails displayed on a wide LCD display screen positioned horizontally, on which multiple miniature robots can move freely. The color sensors beneath the robots can detect and identify lingering “pheromones” on the screen. Meanwhile, the release of any pheromone from each robot is enabled by monitoring its positional information over time with an overhead camera. No other communication methods apart from virtual pheromones are employed in this system. Two case studies have been carried out which have verified the feasibility and effectiveness of the proposed system in achieving complex swarm tasks as empowered by multiple pheromones. This novel platform is a timely and powerful tool for research into swarm intelligence.

**INDEX TERMS** Virtual pheromones, multiple pheromones, bio-inspired, swarm intelligence, micro mobile robots, swarm insects.

## I. INTRODUCTION

Intelligence is one of the remarkable products of natural evolution and is now acknowledged to encompass the concept of swarm or collective behaviors. In nature, swarm or collective behaviors are exhibited in social animals, particularly in social insects which exhibit relatively “simple” neural systems when compared with those of vertebrates. In recent years, such behavior have become source of inspiration for research into swarm intelligence [1], [2]. Within the range of sensory modalities, pheromones are kinds of essential

substances that endow social insects with the capability of working collectively to solve complex tasks and complete large projects [3], [4]. These secreted compounds are exemplified by trail pheromones produced by ants [5] and alarm pheromones released by honeybees [6]. They facilitate direct and indirect communication between individuals leading to the emergence of stigmergic behaviors. These include nest building and food recruitment as observed in ants.

A fundamental feature of these pheromone-based communication is that, insects tend to employ multiple pheromones to achieve higher levels of coordination. Studies show that in addition to releasing the attractant pheromone trails during food recruitment, ants generally release an additional

The associate editor coordinating the review of this manuscript and approving it for publication was Kah Phooi (Jasmine) Seng<sup>ID</sup>.

repellent pheromone [7] to accelerate convergence. At least three functional pheromones are employed by the Pharaoh ant (*Monomorium pharaonis*) during food recruitment [8]. These phenomena indicate that understanding the interactive roles of multiple, rather than single pheromones, may be the key to elucidating more efficient and complex collective behaviors in both biological and robotic swarm systems.

However, compared with single pheromone inspired mechanisms, little attention has been given to multiple pheromones based mechanisms. Although a few modeling studies [9], [10] have utilized multiple pheromones, their mechanisms have verified by simulation only, and not physically in the real world. Comparing the application of real-world models with the in-silico simulation of swarm agents may provide additional insights and to identify differences in these two modes of model implementation [1]. Such studies which use physical robot may provide more convincing evidence of how robust the models are particularly when the input is more noisy and variable. Similar to simulation studies, real robotics studies have also overlooked the potential for exploring the use of multiple pheromones. Although some published studies emulate different pheromones to solve engineering problems, the use of multiple pheromones has not been emphasized as their core focus [11], [12]. Therefore, in this paper we advocate the importance of investigating and exploiting multiple pheromones. To facilitate this approach, a physical multiple pheromone communication platform that permit robotic-pheromone interaction is required.

Given all the facts above, we are proposing a swarm robotic experimental system named ColCOS $\Phi$  shown in Fig. 1. Within this system, one or more pheromones are emulated optically with chromatic tracks displayed on a horizontally positioned screen, upon which multiple miniature ground robots mounted with color sensors can navigate freely. The mounted color sensors face downwards to detect and identify existing “optical pheromones” on the screen. Meanwhile, a monitoring camera collects robot positional information, and a host computer manages the release and evaporation of pheromone track on the screen. In this system, robot agents can run independently, no direct communication is deployed between the host computer and robot agents.

In this study, a series of experiments have been designed using real robots to demonstrate the feasibility of the proposed system, followed by two case studies including a food recruitment task and a behavior mediation task. These bespoke case studies investigate the efficiency, modulation method and robustness of the system. Results from these systematic experiments show that multiple pheromones can be precisely emulated by optical signals. Their functionalities can also be interpreted and reacted correctly by swarm robots in real-time.

The proposed multiple pheromone system provides a powerful tool facilitating the exploration of more complex collective behaviors in both biological [7], [8] and robotic swarm systems, especially in foraging and aggregation. Future research of multiple pheromone mechanism

may play an important role in unraveling the mechanism underlying complex collective behaviors and could potentially provide bio-inspired solutions for challenging problems in swarm robotics. Although pheromone-based algorithms have already been applied to solve realistic tasks [13], challenges still remain. That’s what we believe multi-pheromone based algorithms could help in addressing thus advances the swarm robotics research. For example, multiple pheromone mechanisms may be well suited to solve the exploration tasks in disaster relief scenarios.

The remainder of this paper is organized as follows: Section II provides an overview of relevant background research on pheromones adopted in swarm robotics platforms. Section III describes the details of the proposed ColCOS $\Phi$  system including the emulation of pheromones, and the pheromone release subsystem and the robot platform. Section IV presents preliminary tests to describe the properties and performance of the system. Section V demonstrates the capacity and practicality of the system and is validated by two case studies. Section VI encompasses discussions concerning the wide range of applications of the ColCOS $\Phi$  platform, challenges identified and the recommendations for further research. Finally, the overall conclusions are presented in Section VII.

## II. RELATED WORK

Due to modern low-cost manufacturing technologies, cheaper robots with highly sensitive sensors and powerful computing chips are readily available. This has contributed to the gradual development of swarm robotics from simulation to realistic applications [14], [15]. In the context of the rapid advancement of research into swarm intelligence with the use of physical robots, swarm robotics research is rapidly developing in the areas of aggregation [16], foraging [17], navigation [18], deployment [19], object transportation [20], and education [21], [22]. In the social insect world, such collective behaviors, particularly aggregation and foraging, are dependent on pheromone biology [23]. Thus several previous studies made great efforts to implement pheromones mechanisms in the field of swarm robotics. Approaches can be grouped into four categories.

In the first approach, a “pheromone” is simulated in the form of data in a computer [24] or a chip. This idealized approach has led scholars to question its relevance to the highly complex real world. In [25], the “pheromone” map is updated in the host computer, and then broadcast to the robot through wireless communication, which triggers physical robot interactions in the real physical world. In [26], the “pheromone” is stored as data in RFID chips which are scattered in the environment. The robot acquires and updates the pheromone information by reading from and writing to the chips in close proximity. Although these approaches enable pheromone-like motivation of robot behaviors in the physical world, the key process of the mechanism (e.g. pheromone sensing) still remains as data transmission, which do not reflect limitations of the real physical world.

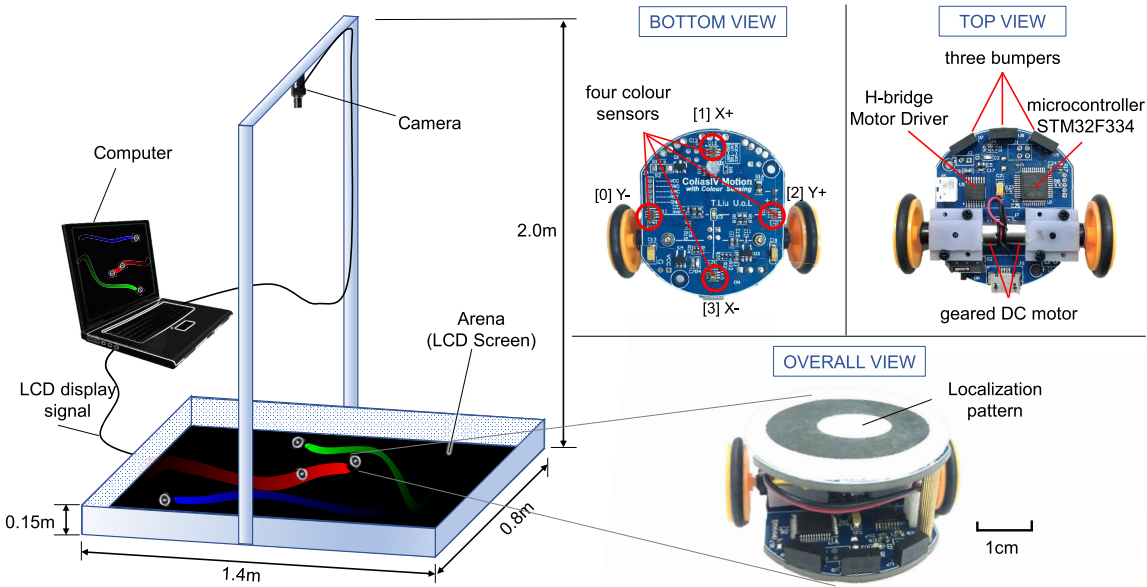


**FIGURE 1.** The ColCOS $\Phi$  system. The camera overhead receives the image containing the patterns attached to the robots. The visual tracking algorithm running in the computer takes this image as input and then outputs the positions of the robots, which is the localization system. The pheromone field (represented by a color image) is calculated in the computer by Eq.(2) or Eq.(5) and updated 30 times per second on the LCD screen, with the protecting wall settling around the screen, it becomes the arena in which the micro-robot explore. Three different views of the micro-robot are shown in the right part of the image.

The second category of attempts is demonstrated in [11], Purnamadjaja *et al.* used combustible substances (alcohol and eucalyptus oil) as artificial pheromones. However, it is difficult to control the evaporation and diffusion of such chemicals in the natural environment, even though this is key to the functionality of real pheromones. Difficulties arise due to wind, temperature, and humidity issues. In addition, such substances are often hazardous due to flammability.

The third way is demonstrated in [27] where the robot drags a heated roller. The heating of the floor to simulate pheromone release. However, this approach also unable to simulate pheromone properties such as evaporation and diffusion. Also, the expenditure of energy is wasteful, and micro robots equipped with only small batteries exhibit very short lifespans.

In the final approach, the pheromone is emulated by light. In examples typical of this optical approach, the virtual pheromone is generated on a defined surface [4], [12], [28] using a ground-positioned or overhead projector. However, due to the large distance between the light source and the imaging surface, ambient light can create interference. In an alternative optical scenario, Kitamura *et al.* [29] have designed a robot that can move around on a touch screen with a pen. The pen “secretes” pheromones onto the screen while color sensors mounted on the robot detect “pheromones” displayed on the screen. This solution can support experiments that involve only a few robots. [30], [31] have designed a system in which a robot shines ultraviolet light onto a paint coated with a photochromic substance, creating virtual “pheromone” trails which decay in intensity. However, the fixed rate of decay is limiting since real pheromones exhibit different evaporation rates.

The most popular solution is to use light as the virtual pheromone [4], [12], [18], [28]–[30], [32]–[34]. Optical methods are highly flexible and can mimic a range of pheromone characteristics. A comparative overview of the preferred and generally popular methods used in implementing virtual pheromones is shown in Table 1. It is clear that optical methods are most tractable and practical for effectively emulating the key characteristics of real pheromone (marking, diffusion, evaporation and diversity), and image display screens are better suited to reducing the impact of ambient light compared with the projection of images onto surfaces, as demonstrated in Arvin’s work [32].

This article focuses on proposing an experimental platform for research into multi-pheromone mechanisms with physical robots. There are a few studies which involve the use of two pheromones in a single task to achieve more complex collective behavior. In [11], Purnamadjaja *et al.* used two pheromones to trigger different behavioral patterns in the robot. However, they used real chemicals (alcohol and eucalyptus oil) as materials to simulate pheromones. Under normal conditions, the chosen sensors are sensitive to both substances. To address this, the authors heated the sensors to different temperatures so that they could distinguish between the two chemicals. However, the authors mention that this approach does not work continuously for extended period. In [12], Simonin *et al.* used multi-pheromones for exploration and transport tasks. Kitamura *et al.* [29] used a home pheromone and a food pheromone to build a pheromone gradient map to navigate the robot to and from the home and food source. In our previous conference papers [19], [33], we presented the preliminary multiple pheromone experimental platform with brief case studies, but its performance

and scope were not investigated due to the limited length of the conference papers. In this study, we further demonstrate and test the platform systematically in the following parts.

In summary, this paper presents a platform capable of simultaneously emulating multiple pheromones. Compared with other multi-agents platforms such as ARK [25] and Kilogrid [35], this platform is more affordable and intuitive as the pheromone is emulated in a visible way.

### III. THE ColCOSΦ PLATFORM

The pheromone communication system proposed in this paper is named ColCOSΦ where “Col” stands for “Color”, “COS” is the abbreviation of “Communication System” and “Φ” stands for “pheromone”. This platform is designed specifically for studying pheromone-controlled collective behaviors which based on the pheromone interactions of social insects. The ColCOSΦ system is shown in Fig. 1, and consists of two subsystems and one specially designed micro robot platform:

- A pheromone distribution emulation system: The pheromones’ distribution in the environment is modeled as a map which is stored in a host PC that is kept updating according to the pheromones’ physical characteristics. An LCD screen settled horizontally is employed to display the pheromones’ distribution by three color channel.
- A pheromone releasing emulation system: a monitoring camera is hang above the arena to grab images of the full experiment. Locations of individual robots are detected and tracked in real-time by an efficient image-based localization algorithm running in the host PC to emulate pheromone’s releasing functions (see Fig. 1).
- Micro robot platform: A micro robot platform is developed to detect the optically emulated pheromones from the bottom side with several color sensors when running on the LCD screen.

These three subsystems are described in detail below:

#### A. THE PHEROMONE DISTRIBUTION EMULATION SYSTEM

##### 1) WHAT IS PHEROMONE

Pheromone is a biochemical signaling compound that is released by an organism to facilitate direct and indirect communications [3], [4]. With the aid of pheromones, animals can cooperate with each other to complete complex tasks that are impossible for a single agent to achieve. Coordination with pheromones thus forms the foundation of stigmergic behaviors in many insects such as ants [5] and bees [6].

This mechanism has three major differences comparing to the direct radiation-based communication methods (including radio, sound or light-modulated signals). First, pheromones are released and then disappear at the original location at a certain temperature, resulting in a delayed effect. This means the information can be received by

another agent in the future. Moreover, the delayed time can also be increased if pheromones are released several times. Second, the environmental conditions information such as terrain accessibility, temperature and wind can also be conveyed by the fluctuations and distribution of pheromones. Third, the information is “anonymous” and collective, which means multiple pieces of information can be sent to a single agent without an extra computation process.

To emulate pheromones correctly and effectively, several fundamental characteristics which determine their ability to transmit information in the environment must be addressed, involving *marking*, *diffusion*, *evaporation* and *diversity* [28]. Therefore, a virtual pheromone system should present the pheromone in the environment precisely like a marker, and the spatiotemporal change over time of the virtual pheromone should replicate the diffusion and evaporation properties. Last, but not least, the system should be capable of simulating different kinds of pheromones to allow complex and diverse communications.

#### 2) PHEROMONES EMULATION AS COLOR IMAGE

In this system, the goal is to emulate three kinds of pheromones simultaneously. Thus, the virtual pheromone field is modeled as a map with a depth of three (i.e., a color image) and defined by a  $W \times H \times 3$  matrix  $\mathbf{I}$ , where  $W$  is the width and  $H$  is the height. All pixels of the image collectively emulate the distribution of gas molecules of which a real pheromone field is comprised, spreading along the  $X$  ( $x \in N^+$  and  $0 \leq x < W$ ) and  $Y$  ( $y \in N^+$  and  $0 \leq y < H$ ) axis. Within the modeled pheromone field, the color ( $c$ ) of a pixel corresponds to the  $i^{th}$  type of the pheromone, and the brightness ( $I(x, y, c)$ ) of a pixel corresponds to the concentration  $\Phi_{i,j}$  of the pheromone. Given that there are three primary color channels (i.e., red, green and blue, thus  $c \in \{r, g, b\}$ ), this virtual pheromone system can represent a pheromone field containing a maximum of three kinds of pheromones. Therefore, the color image can be constructed by the following equation

$$\mathbf{I}(x, y, c) = \sum_{j=0}^N k_{i,j} \Phi_{i,j}(x, y) \quad (c, i) \in \{(red, 0), (green, 1), (blue, 2)\} \quad (1)$$

where the scale factor  $k_{i,j}$  modulates the contribution of the  $i^{th}$  type of  $j^{th}$  pheromone to the color image.

Thus, the pheromone *marking* characteristics is simulated by the pixels of the image and the *diversity* or type of pheromone is simulated by the pixel color ( $c$  in Eq.(1)). Similarly, the realization of other crucial characteristics of the pheromone (i.e., the *diffusion* and *evaporation*) are implemented by the updating of the color image. This is modeled as a differential equation:

$$\dot{\Phi}_{i,j}(x, y) = -\frac{1}{e_{\Phi_{i,j}}} \Phi_{i,j}(x, y) + d_{i,j} \Delta \Phi_{i,j}(x, y) + J_{i,j}(x, y) \quad i \in \{0, 1, 2\}, j = 0, 1, \dots, N \quad (2)$$

**TABLE 1.** Comparison of implementations of virtual pheromone.

Substance	Method	Corresponding Sensor	Multiple pheromone	Extra Description
Optics	Localization system and projector [12], [28]	Color sensor / color camera	[28] Possible [12] Yes	Controllable. Flexible to modify parameters of evaporation, diffusion. <b>Unstable to the ambient light.</b>
	Localization system and screen [32]–[34]		[32], [34] Possible [33] Yes	<b>Controllable, stable, flexible to modify parameters of evaporation, diffusion.</b>
	Pen and touch screen [29]		Yes	Controllable, stable, flexible to modify parameters of evaporation, diffusion. <b>Limited number of robots and unable to identify different robots</b>
	UVLED and phosphorescent glow-paint [30], [31]		NO	Not very controllable and hard to modify the parameters. Working in a dark environment.
Heat	heater [27]	temperature sensor	NO	<b>Impractical for small robots, energy-consuming.</b>
Data information	IR communication [18]	data sender and receiver	Possible	Cannot implement all the properties of pheromone.
	Localization based virtual environment [25], [35], [36]		Possible	Pheromone information is calculated and stored in a central computer. <b>No direct interactions with robots.</b>
	RFID tags [26], [37], [38]		Possible	Very different to implement all the properties of pheromone.
Chemical substances	ethanol [39], eucalyptus oil [11]	gas sensor	Yes	<b>Not very controllable, impractical for micro-robots.</b>

where:

- **Marking:**  $J_{i,j}(x, y)$  is the initial pheromone injection at position  $(x, y)$ . This can be either the current position of the robot that releases the pheromone, or the position where the source of the pheromone designed to be deposited.
- **Evaporation:**  $e_{\Phi_i}$  is the evaporation factor which defines the rate of the exponential decay of the pheromone strength over time.
- **Diffusion:**  $d_{i,j}$  is the diffusion factor and together with the spatial rate of change in the strength of the pheromone ( $\Delta\Phi_{i,j}(x, y)$ ) calculated by Eq.(3). Equation (4) for the horizontal ( $h$ ) and vertical ( $v$ ) directions respectively.) which determines how the pheromone spreads spatially.

$$\Delta\Phi_{i,j}(x, y) = \Delta\Phi_{i,j}(x, y)_h + \Delta\Phi_{i,j}(x, y)_v \quad (3)$$

$$\begin{cases} \Delta\Phi_{i,j}(x, y)_h = (\Phi_{i,j}(x - 1, y) - \Phi_{i,j}(x, y))/2 \\ \Delta\Phi_{i,j}(x, y)_v = (\Phi_{i,j}(x, y - 1) - \Phi_{i,j}(x, y))/2 \end{cases} \quad (4)$$

The differential equations determine the trend of the pheromones over time, but it is difficult to foresee the final status. There is an additional method that can be used to model the pheromone in a spatiotemporal way which can be made by solving Eq.(2). By applying the scaled bivariate normal distribution and the exponential decay function, the pheromone can be expressed by:

$$\begin{aligned} \Phi_i(x, y, t) &= \frac{K_i}{2\pi\sigma_{x_i}\sigma_{y_i}\sqrt{1-\rho_i^2}} \cdot e^{-\frac{t}{e_{\Phi_i}}} \\ &\cdot e^{-\frac{1}{2(1-\rho_i^2)} \left[ \frac{(x-\mu_{x_i})^2}{\sigma_{x_i}^2} + \frac{(y-\mu_{y_i})^2}{\sigma_{y_i}^2} - \frac{2\rho_i(x-\mu_{x_i})(y-\mu_{y_i})}{\sigma_{x_i}\sigma_{y_i}} \right]} \end{aligned} \quad (5)$$

where for:

- **Marking:**  $\mu_x$  and  $\mu_y$  define the position at which the pheromone is injected, which has the same physical

meaning as  $J_{i,j}(x, y)$  in Eq.(2).  $K_i$  is a scaling factor to determine the changes in strength of the pheromone.

- **Evaporation:**  $e_{\Phi_i}$  is the evaporation factor which defines the rate of the exponential decay of the pheromone strength over time  $t$ .
- **Diffusion:**  $\sigma_{x_i}$  and  $\sigma_{y_i}$  are diffusion factors determining the rate at which the pheromone spreads in the  $x$  and  $y$  directions respectively.  $\rho_i$  validates the basic different spatial diffusion in the  $x$  and  $y$  directions, which can be used, in some circumstances, to model the effect of wind on diffusion.

Note that this model constructs the whole pheromone field, thus Eq. (1) becomes:  $I(x, y, c, t) = k_i\Phi_i(x, y, t)$ .

The Eq.(2) and Eq. (5) can be selected to model the pheromone according to requirements of the application since both of them can replicate all the crucial characteristics of pheromone. The differential equation Eq. (2) has a better dynamic performance and can be easily implemented by iteration whilst the Eq. (5) is more intuitive and make it easier to speculate as to the stable shape of the pheromones' distribution.

### 3) DISPLAYING VIRTUAL PHEROMONES ON A SCREEN

First, a host PC (CPU: Intel i5-10500 @ 3.1GHz, RAM: 16GB @ 2666MHz in our implementation) constricts a optically-simulated virtual pheromones' distribution map. Then, the distribution map is displayed on a high resolution (4K) 65-inch color LCD screen (1.43 m in length and 0.81 m in width). The flat screen is positioned horizontally and serves as the arena for the robots as shown in Fig. 1 (left side). The resolution of the map is set to  $1920 \times 1080$ , hence a single pixel is scaled at  $75\mu\text{m} \times 75\mu\text{m}$ , which is small enough to precisely emulate the pheromone molecule unit whilst the robot has a diameter of 4 cm. The resolution of the map is adjustable for a good balance between accuracy and time consumption. Practically, a resolution of  $1920 \times 1080$  consumes around

230 ms to complete a full update process. A plastic wall that retains micro-robots is mounted around the screen, defining the boundaries and protection of the arena.

### B. THE PHEROMONE RELEASING EMULATION SYSTEM

Since the robot cannot literally leave a physical trail on the screen, the host PC is responsible to “draw” pheromone trails for robots according to their locations. So, the real workflow of the host PC is 1) localizing the every robots’ position by recognizing specific visual patterns (see Fig. 1) pasted on the top of the robots, and as different robots could carry different patterns so that individual robot can be identified; 2) updating the pheromone field according to the pheromone model ((2) and (5)) and the customized settings; 3) transferring the pheromone field to a color image and then displaying the image on the horizontal screen.

#### 1) ROBOT DETECTION AND LOCALIZATION

In order to capture the positions of multiple robots in real-time while moving around, an efficient image-based algorithm is applied. The fundamental idea of this algorithm is to detect a unique ring-style recognition pattern (see Fig. 1, right hand side) carried on top of all the robot [40]. By detecting the position of all the visible ring patterns, the locations of all robots can be tracked fast. The ring pattern uses two ellipses with varied long axis inclinations to discriminate different IDs and use the eccentric angle to determine the whole pattern’s orientation. The fast detection of ring patterns is realized by a flood-fill algorithm that can filter out all possible rings, followed by a rule-based method to allocate pre-assigned IDs to each of the matched patterns.

#### 2) COORDINATES TRANSFORMATION FOR PHEROMONE PROJECTION

In the proposed platform, robots and its pattern are exist in the 3D space so that the position of the pattern can be described as a 3D coordinate in the world canonical coordinate. To correspondence the world and the virtual pheromone map coordinate, the coordination transformation is need. To maintain uniformity, all three coordinate systems in our system(see Fig. 2) are maintained using 3D coordinate form, they comprise:

- $[X_c, Y_c, Z_c]^T$ : The image coordinate of the camera in the localization system.
- $[X_w, Y_w, Z_w]^T$ : The world coordinate measuring the robots and the arena.
- $[X_p, Y_p, Z_p]^T$ : The screen display coordinate which represents the pheromone field map.

The pattern determined by the image coordinates is transformed into the camera centered coordinate frame in a canonical camera form. The canonical camera is modeled as the ideal pinhole camera with no radial distortions (for further details see [40]). We can transform the image coordinates to world coordinates by simply multiplying with a  $3 \times 3$  transformation matrix  $\mathbf{H}$  shown in Eq.(6). The transformation matrix

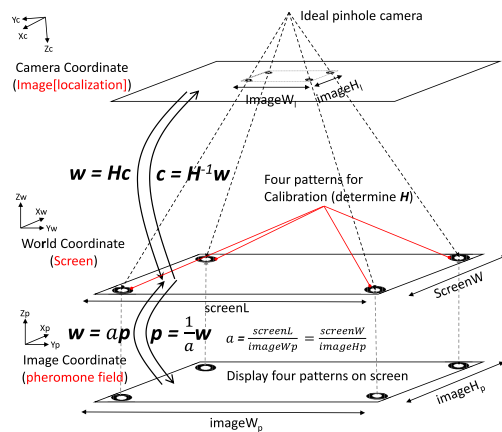


**FIGURE 2.** The three coordinate systems and their mutual transformation.

$\mathbf{H}$  can be defined by placing at least three “calibration” patterns in the camera field. In our case, four independent “calibration” patterns (Fig. 2) are displayed on the screen and group as four triplet to calibrate the transformation matrix  $\mathbf{H}$  for increasing system accuracy. In addition, the pattern moves on a 2D flat plane over 5cm (robot-height) of the screen, so the canonical coordinate of image and world can be described as homogeneous spatial coordinates  $[x_w, y_w, 1]^T$ , and the transformation equation can be represent as Eq.(7).

$$\mathbf{w} = \mathbf{Hc} \quad (6)$$

$$\begin{bmatrix} x_w \\ y_w \\ 1 \end{bmatrix} = \begin{bmatrix} h_{11} & h_{12} & h_{13} \\ h_{21} & h_{22} & h_{23} \\ h_{31} & h_{32} & h_{33} \end{bmatrix} \begin{bmatrix} x_c \\ y_c \\ 1 \end{bmatrix} \quad (7)$$

As for the transformation from the pheromone field to the screen, we simply bring them into alignment to make them aligned. There is only a scaling factor  $a$  (Fig. 2) contained in this transformation. The scaling factor can be determined by the ratio of the image width (or height) in pixels to the screen length (or width).

Although we can achieve the correspondence between the world coordinates and the virtual pheromone map coordinates by the above 2D coordinate transformation, it is necessary to use 3D coordinates to represent the position of the pattern. As the localization subsystem can localize pattern positions in 3D space, retaining the position information expressed in 3D coordinates leaves the possibility for the platform to experiment in an arena with fluctuating terrain.

### C. THE MICRO-ROBOT PLATFORM

One of the key component to utilize this system is the micro-robot platform which can detect, identify and react to the optically emulated pheromones on the screen. We have designed an ideal micro-robot platform based on the Colias-IV robot prototype which is a differential driven ground robot featured with small in size, light-weight and strong computing power [41]. However its original sensory peripherals is not capable of detecting color information, substantial modifications and improvements need to be adopted

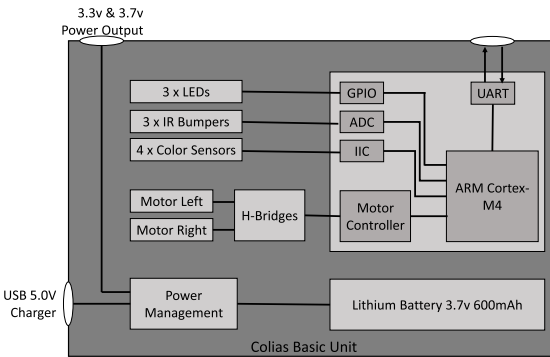


**FIGURE 3.** The schematic diagram of the hardware connections of the robot.

by adding four highly sensitive multi-channel optical detectors that face to the bottom side to pickup intensity of red, green and blue separately. The four color sensors are arranged in a diamond shape to detect the gradient of light intensity, as shown in Fig. 1.

The hardware architecture of the robot is shown in Fig. 3. In contrast to the previous Colias generation, the micro-control unit (MCU) in the new robot is upgraded to the STM32F334. The new MCU has stronger computing resources, as well as more communication interfaces and IO ports, enabling it to meet the increased requirements for sensor data collection and motor control. Besides, the brightness sensor used in the previous generation has been replaced by the color sensor TCS34725, which uses a 12-bit high-precision ADC to separately capture the brightness of the three color channels, red, green and blue, and then send the data to the micro controller via the Inter-Integrated Circuit (IIC). Three reflective infrared bumper sensors are installed at the forefront of the robot to detect nearby obstacles. Two motors are driven by a compact two-channel H-bridge controlled directly by Pulse-width modulation (PWM) signals generated by the MCU.

The proposed platform works with the improved Colias-IV micro-robot for best adaptability. It can also be used along with other micro-robots such as e-puck, Jasmine or customized micro-robots, if the selected robot can detect and measure the intensity of red, green and blue channels separately from the bottom side. In the situation that these sensors are not integrated into the robot's body, one work-around is to attach an extension module to the robot and connect to it with a two-wire communication protocol called IIC, which should have been provided by most of the micro-robots.

#### D. INTERACTION WITH EMULATED PHEROMONES OF ROBOTS

To interact with multiple pheromones emulated on the screen, a robot need to discriminate the direction of gradient. Meanwhile, control strategies relied on the pheromone information also need to be designed. In this section, the calculation of pheromone's gradient and two robot control strategies are

proposed, which are 1) to react to the attractive and repulsive pheromones and 2) to follow and trace a pheromone trail.

#### 1) PHEROMONES GRADIENT CALCULATION

As shown in Fig. 1 (underside view of the robot), the Cartesian coordinate system uses the center of the robot as the origin, and the front and left as the positive directions of the X-axis and Y-axis respectively. Thus, the  $0^\circ$  direction of the coordinates system is aligned with the forward direction in front and ahead of the robot. The four color sensors are defined as  $n \in \{0, 1, 2, 3\}$ . The direction of the gradient is calculated by:

$$\theta_i = \arctan \frac{\phi_{i,2} - \phi_{i,0}}{\phi_{i,1} - \phi_{i,3}} \quad (8)$$

where  $i^{th}$  color light intensity stands for the strength of the  $i^{th}$  type pheromone  $\phi_{i,n}$  ( $i = \text{red, green, blue}$ ). The overall pheromone strength  $\phi_i$  sensed by the robot at its current position is defined as the average strength of its four sensors.

#### 2) GRADIENT TRACKING AND AVOIDANCE

Tracing an attractive or avoiding a repulsive odor source is ubiquitous in the animals' kingdom. Similarly, for robots, reacting to pheromones with opposite purposes also provide unique opportunities to emulate and study real-world olfactory sensing and social animal behaviors.

As previously described, the gradient can be easily calculated by Eq. (8). After elucidating the direction of a pheromone gradient, the desired direction of movement can be determined by Eq. (9):

$$\mathbf{M}_a = (\phi_a, \theta_a), \quad \mathbf{M}_r = (\phi_r, \theta_r + \pi) \quad (9)$$

where  $\phi_a$  and  $\phi_r$  defines the strength of the detected attractive or repellent pheromone respectively, and  $\theta_a$  and  $\theta_r$  denote the directions of the positive gradients. Note that the desired direction for movement is the same as the positive gradient direction for an attractive pheromone ( $M_a$  in Eq.(9)) but opposite (offset  $\pi$ ) for a repellent pheromone ( $M_r$  in Eq.(9)).

In more realistic situations, several different pheromones may be detected simultaneously. Therefore, a cue integration mechanism is needed. Here we have applied a bio-inspired method to carry out the optimal integration of circular cues which is based on a ring attractor neural network architecture [42]. In our case we have used the mathematical format of this method known as vector summation as described in [43]. Hence, the integrated motion direction ( $\theta$ ) can be obtained by vector summation  $\mathbf{M} = \mathbf{M}_a + \mathbf{M}_r = (M, \theta)$  and  $\theta$  is calculated by Eq.(10):

$$\theta = \arctan \frac{\phi_a \sin \theta_a + \phi_r \sin(\theta_r + \pi)}{\phi_a \cos \theta_a + \phi_r \cos(\theta_r + \pi)} \quad (10)$$

The desired direction of motion is used to determine the rotational speeds ( $\omega_l$  and  $\omega_r$ ) of the robot's left and right motors, which can be defined by Eq.(11):

$$\begin{cases} \omega_l = v_b - \alpha\theta \\ \omega_r = v_b + \alpha\theta \end{cases} \quad (11)$$

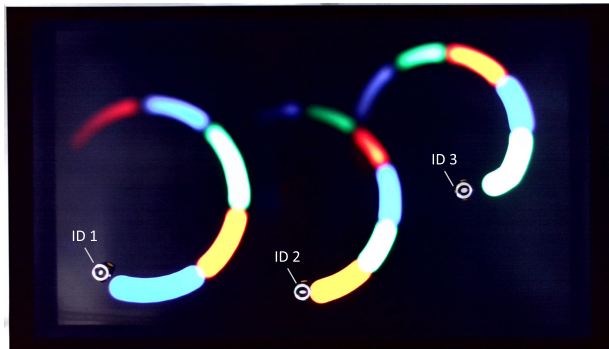


**FIGURE 4.** Snapshot of the designed experiment demonstrating the proposed platform enables different agents to release different pheromones at the same time and also allows one agent to release different pheromone at different times.

where  $v_b$  represents the initial forward speed, generally set to 4-5 cm/s, and  $\alpha$  is the parameter for adjusting the reactive rotation motion.

### 3) PHEROMONE TRACING AND FOLLOWING STRATEGY

Another fundamental ability required by the robot is to follow the pheromone trails precisely inspired by the ants [44]. The algorithm described below shows the trail tracking motion control strategy.

## IV. FUNCTIONALITY AND PERFORMANCE OF ColCOSΦ

A series of experiments are designed to verify the effectiveness, and to evaluate the performance of the ColCOSΦ system. The basic functionalities are firstly tested, including the pheromones' emulation and releasing of the platform and the pheromones perception and reactive control of robots. Following by two realistic behavioral studies to evaluate the trail following and gradient tracking features with different control strategies.

### A. BASIC FUNCTIONALITIES

#### 1) PHEROMONES' EMULATION OF ColCOSΦ

In order to assess the capability of the ColCOSΦ system to 1) dynamically release pheromones according to the positions of the robot and 2) to emulate the evaporation and diffusion effect of pheromones; 3) identify individual robot via the specific pattern, we assigned with a pheromone configuration to see whether pheromones are emulated realistically and efficiently on the screen. An experiment designed that three robots with different IDs (with different pattern pasted) move in circles in the arena. Each of these three robots release one of three different types of pheromones (displayed as red, blue and green) in a constant time interval (3 seconds) and then switch to another one and repeat this procedure. Note that at each time, three robots could release different kind of pheromone as showed in Fig. 4, demonstrating the localization system could identify individual agent and each agent could release different pheromones. Furthermore, the successful release of the pheromones modeled by Eq.(2) is

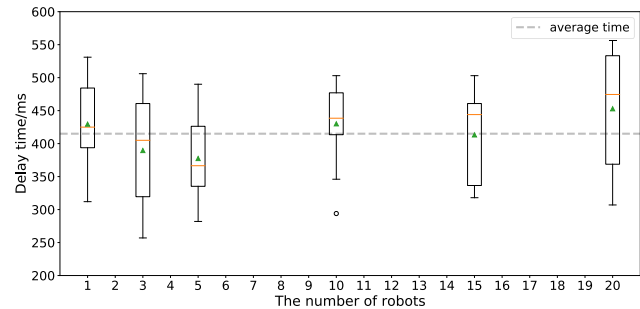


**FIGURE 5.** Time delay versus different number of robots. The gray line shows the average time of the test. The green triangles show the average times of each group. It suggests that the number of robots does not correlate well with the time delay when the robot number less than 20.

shown by the different colored tails behind the robots. The robots draw circles at speeds of approximately 6cm/s, the distance between robot and the pheromone trails is approximately 3cm.

This delay length results from that the host PC need time to grab images, calculate the location and pheromones field, transfer pheromone map to the LCD screen. When the pheromone field resolution set as  $1920 \times 1080$  and 3 robots move in the arena. The PC typically consumes approximate 413ms and 110MB memory. When those parameters set as  $3840 \times 2060$  and 3 robots. The PC typically consumes approximate 1107ms and 219MB memory. The results of time delay tests at resolution of  $1920 \times 1080$  with different numbers of robots are shown in Fig. 5. It suggests that the time delay does not correlate well with the number of robots but with the resolution of the pheromone field. So the resolution of pheromone field is set as  $1920 \times 1080$  and it is precise enough to transfer pheromone information to the robots.

To further investigate the performance of pheromone release and the pheromone emulation models realized by Eq.(2) and Eq.(5), Several groups of configurations containing varied parameters - the evaporation ( $e$  in Eq.(2) and Eq.(5)) and diffusion ( $d$  in Eq.(2) and  $\sigma_x, \sigma_y$  in Eq.(5)) are employed and tested. The results are shown in Fig. 6 and Fig. 7. When the evaporation factor  $e$  is increases, the pheromone evaporates at a slower rate, resulting in a longer pheromone tail (Fig. 6 top images, Fig. 7, top images). Similarly, the pheromone possessing a higher diffusion factor will spread around faster, resulting in a wider pheromone spot when given a certain time window (Fig. 6 bottom images; Fig. 7 bottom images).

The results of experiments above show that the proposed ColCOSΦ system can simulate the pheromone releasing function and simulate the dynamic evaporation and diffusion properties correctly.

#### 2) PHEROMONES' DETECTION AND REACTIVE CONTROL OF ROBOTS

One of the most important features of the designed micro-robot platform is the detection, discrimination and

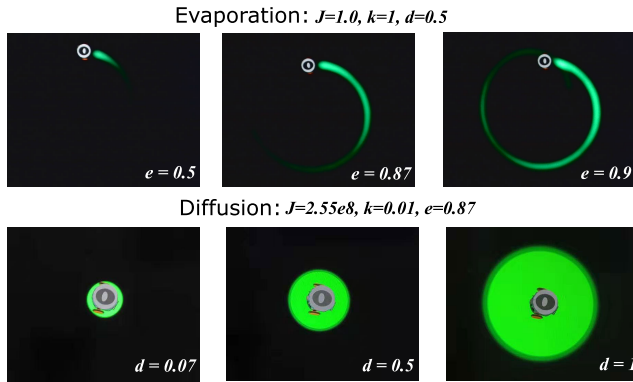


**FIGURE 6.** The comparison experiments exploring the pheromone modeled by Eq.(2).

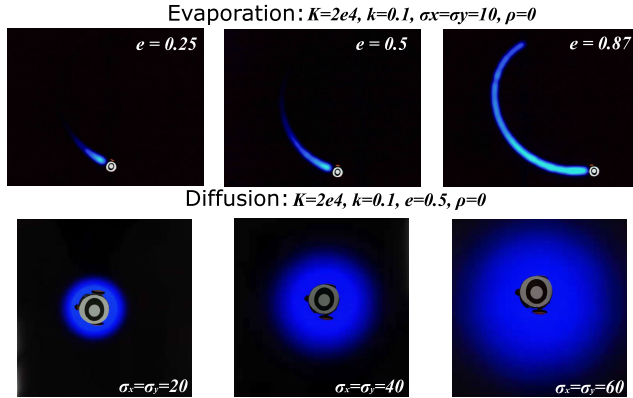


**FIGURE 7.** The comparison experiments exploring the pheromone modeled by Eq.(5).

intensity measurement of different colors displayed on the screen which represent pheromones. To evaluate the performance of the color sensing features, one robot is placed on a row of color blocks displayed on the screen where the colors is described by 8-bit RGB color space. The measured color intensities of red, green and blue channels of all the four sensors are then recorded and plotted. The Fig. 8 illustrates the results of measured color intensities responding to the gradually increasing red solely. The perceived colors increase almost linearly as expected when the displayed brightness is greater than 50. It should be noted that the blue and green channels also respond to red color display due to the LCD's natural characteristics, yet this minor coupling is acceptable.

All together, the basic functionalities of ColCOS $\Phi$  are reliable for carrying on relevant research in the context of swarm robotics and social insects.

## B. THE PROPOSED BIO-INSPIRED CONTROL STRATEGY

In this subsection, two examples are used to demonstrate the basic robot control strategy inspired by observed behaviors of animals.

### 1) GRADIENT TRACKING AND AVOIDANCE

Examples of the robot's pheromone tracking and avoidance capabilities are illustrated in Fig. 9. The attractive pheromone

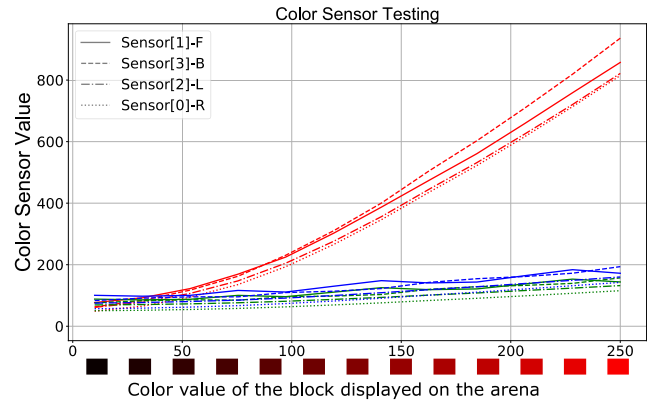


**FIGURE 8.** The performance of the four color sensors mounted in the robot reading the RGB channel of red blocks.

is denoted by a blue circular field whilst the repulsive pheromone is shown by a red circular field (see Fig. 9). These pheromones are rendered according to Eq.(5). The robots are initially placed in random positions at the edge area of the attractive pheromone field or the inner area of the repulsive pheromone field. Accordingly, the behavior of tracing by the attractive pheromone or avoidance to the repulsive pheromone are aroused. The trajectories of robot in either cases are shown in Fig. 9 which clearly show that robots are capable of reacting to different types of pheromones according to the aforementioned control strategies.

It is worthwhile to mention that, the motion performance can be tuned by adjusting  $\alpha$  in Eq.(11). When  $\alpha$  is decreased slightly, the steering adjustment may not be sufficient, leading to the curved trajectories as shown in the top-left part of Fig. 9. This spiral path is interestingly reminiscent of the Logarithmic spiral of a moth flying towards a light source. On the other hand, the shape of the initial path to avoid the repellent pheromone is not regular due to the arbitrary initial headings of the robot. Nevertheless, the performance for fleeing from the repellent pheromone site is respectable (right part of Fig. 9 top).

### 2) PHEROMONE TRAIL FOLLOWING PERFORMANCE

To test the capability of the robot to maintain a stable trace following behavior, four different patterns following tests are conducted. The patterns composed by pheromone trails are shown in Fig. 11: a circle, a straight line, a fork-shape path and a tortuous route, all with a width of 2.5cm which is slightly less than the gap between the left and right color sensors. This ensures that for the most part the left and right sensors will have a low readout since facing the black background out of the trails whilst the front and rear sensors will have very high readout values (see Fig. 10 for the specific control strategy). Algorithm. 1 shows the details of the control logic where the  $2^\circ$  and  $10^\circ$  is selected for adjusting the robots' heading according to whether the front sensor is on the trail (i.e., whether the value of the sensor output is lower than the threshold). These two parameters are empirical

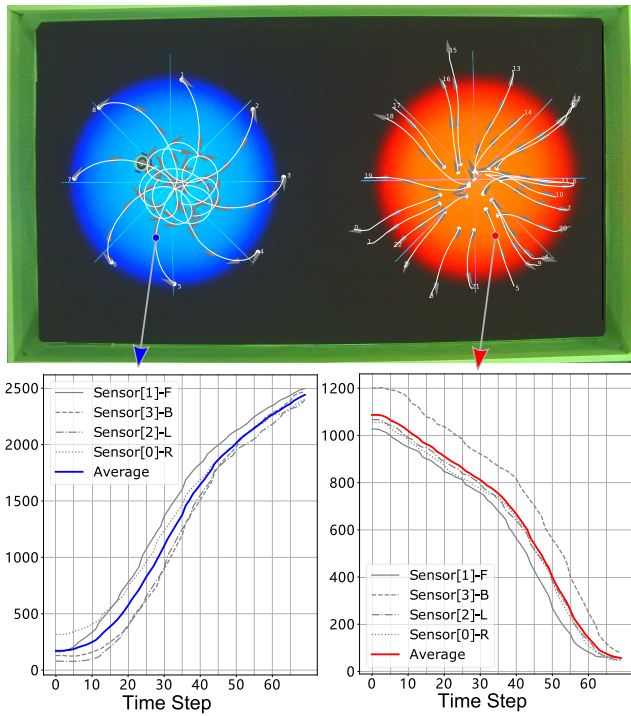


**FIGURE 9.** Demonstration of robotic tracking of the attractive (blue) pheromone source and avoidance of the repulsive (red) pheromone source. The white lines show the trajectories of the robots released at different initial positions (marked by white dots). The gray arrows depict the moving direction of the robot on the route. The values of the color sensors of two agents during the tracking and avoidance are shown in the graphs below.

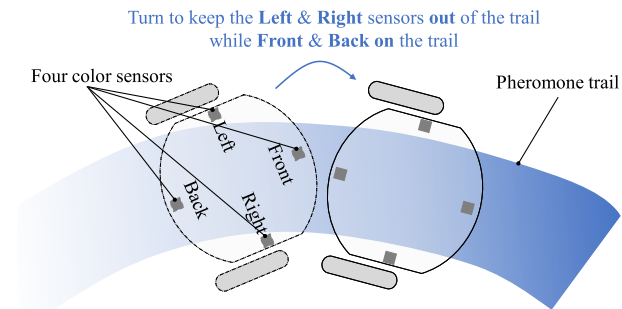


**FIGURE 10.** Schematic diagram to illustrate the capability of the robot control to follow the trail of the pheromone.

values determined by the robot's motion characteristics and the control interval.

Note that the metric to evaluate the performance of the trail following is decided by the position error ( $\epsilon$ ), calculated by:

$$\epsilon = \frac{1}{N} \sum_{i=0}^N \sqrt{(x_i - XT_i)^2 + (y_i - YT_i)^2} \quad (12)$$

where  $x_i, y_i$  provide the position of the robots as measured by the localization system,  $XT_i, YT_i$  are the positions of the

---

### Algorithm 1: Pheromone Trail Following Control Strategy

---

```
// Define rotation to the left as positive
while robot power on do
    if no obstacle detected then
        if the front sensor on the trail // see Fig.10
        then
            if the left sensor on the trail then
                Set motors' speed to turn a 2° angle;
            else if the right sensor on the trail then
                Set motors' speed to turn a -2° angle;
            else
                Set motors' speed to go Forward;
        else
            if the left sensor on the trail then
                Set motors' speed to turn a 10° angle;
            else if the right sensor on the trail then
                Set motors' speed to turn a -10° angle;
            else
                Collision avoidance;
    delay 50ms;
```

---

**TABLE 2.** The performance of trail following.

Trail No.	Shape	N	$\epsilon$ (mm)
1	Circle	200	3.87
2	Line	200	2.95
3	Fork	300	4.17
4	Tortuous	500	4.49

points sampled from the pheromone trail and  $N$  is the number of measurements.

In all the four tests, the position error  $\epsilon$  is less than 5mm (see Table. 2). The trajectories of the robot, shown in red lines in Fig. 11, coincide precisely with the pheromone trails it follows. The ability to follow the fork-shaped path demonstrates the capability of preliminary decision-making at the bifurcation point. Note that for the trails that are not closed (i.e., the fork and the straight line), the robot's ability to turn around at the end of the trail is spontaneously enabled by the controlling strategy that ensures the front sensor being kept within the trail (Algorithm. 1).

To sum up, the two presented examples have demonstrated the effectiveness and precision of the proposed system co-ordinating every subsystems with control strategies in multiple pheromone based implementation.

## V. CASE STUDIES

In this section, to further investigate the capabilities, effectiveness and efficiency of the ColCOSΦ artificial multiple pheromone system, and to provide an indication of the

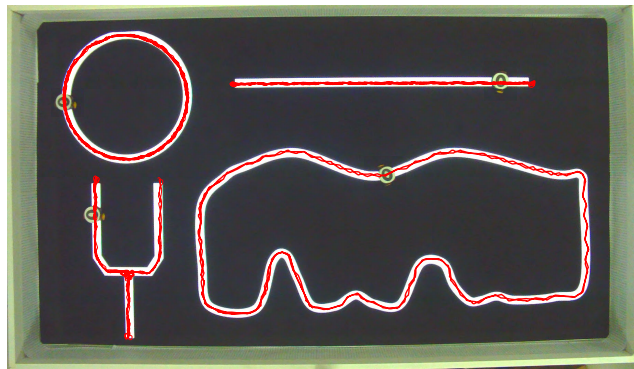


**FIGURE 11.** Demonstration of the capability of the robot to follow differently shaped pheromone trails. Four examples are displayed in the figure. The trajectories of the robots are shown as red lines. Position error is less than 5mm throughout (see Table. 2).

research opportunities it may bring, we report two case studies, the designs of which are based on observations of social insects, and desired performance in complex physical scenes.

#### A. FOOD RECRUITMENT TASK—HOW DO MULTIPLE PHEROMONES IMPROVE EFFICIENCY?

Three different kinds of pheromones have been implicated in food recruitment by ants, thus highlighting the importance of research into multiple pheromones. Inspired by this biological study, we have designed and carried out an experiment that involves all three pheromones.

##### 1) PHEROMONE FIELD CONSTRUCTION

The process of forming a pheromone network from a completely initial state is a very complex task for micro robots in foraging. To focus on the impact of the multiple pheromones, we started the experiment from the food to nest paths have been established preliminarily. In this experiment, so as to understand the fundamental way in which pheromones dictate the agents' behaviors, and to optimize the use of our system, the pheromone trails and branches have been designed according to the experimental requirements. According to previous research [7], the three kinds of pheromones are:

- Long-term attractive pheromone (LAP) marks the trails from the nest to the potential food sites, depicted in Fig. 12 as the blue trails.
- Short-term attractive pheromone (SAP) is released to convey up-to-date information of the presently available food sources. This pheromone is drawn with the green color but mixes with the blue to give cyan in Fig. 12.
- Short-term repellent pheromone (SRP) is released at the bifurcations to close off the unrewarding branches. This pheromone is drawn with the red color which mixes with the blue to give magenta in Fig. 12.

The pheromones' physical effects modeled by Eq.(2) is employed in this case. According to the experimental requirement that a stable path-network formed by pheromone trails is

**TABLE 3.** Pheromone parameter setting in case study A.

Type	Color	Model	Evaporation	Diffusion	Injection
LAP	Blue	Eq.(2)	$e_{\Phi_{i,3}} = 50s$	$d_{i,3} = 0$	$J_{i,3} = \mathbf{D3}_i$
SAP	Green	Eq.(2)	$e_{\Phi_{i,2}} = 50s$	$d_{i,2} = 0$	$J_{i,2} = \mathbf{D2}_i$
SRP	Red	Eq.(2)	$e_{\Phi_{i,1}} = 50s$	$d_{i,1} = 0$	$J_{i,1} = \mathbf{D1}_i$

needed, we applied a larger evaporation period and a smaller diffusion coefficient. The parameters settings are listed in Table. 3, where  $\mathbf{D1}$ ,  $\mathbf{D2}$ ,  $\mathbf{D3}$  are  $W \times H$  metrics that define the strength at each position across the whole pheromone field. The constructed pheromone fields are shown in Fig. 12. Note that the cyan trail is a mixture of blue (LAP) and green (SAP) pheromones, and similarly the magenta trail is a mixture of blue (LAP) and red (SRP) pheromone.

Three different pheromone field layouts, combining different numbers and types of pheromone are shown in Fig. 12 representing three different experimental groups, G1-G3, as listed below:

- G1: robot forages with only the LAP.
- G2: robot forages with both the LAP and the SAP.
- G3: robot forages with all the three pheromones.

These three groups are designed to compare the efficiency with which agents are able to find the correct food sites. The simulated ants (i.e. the robots) should respond differently to the different types of pheromones (see Section V-A2 for details). The improvement in efficiency results from the use of multiple pheromones that can be visibly deduced from the results across the groups.

##### 2) ROBOT CONTROL

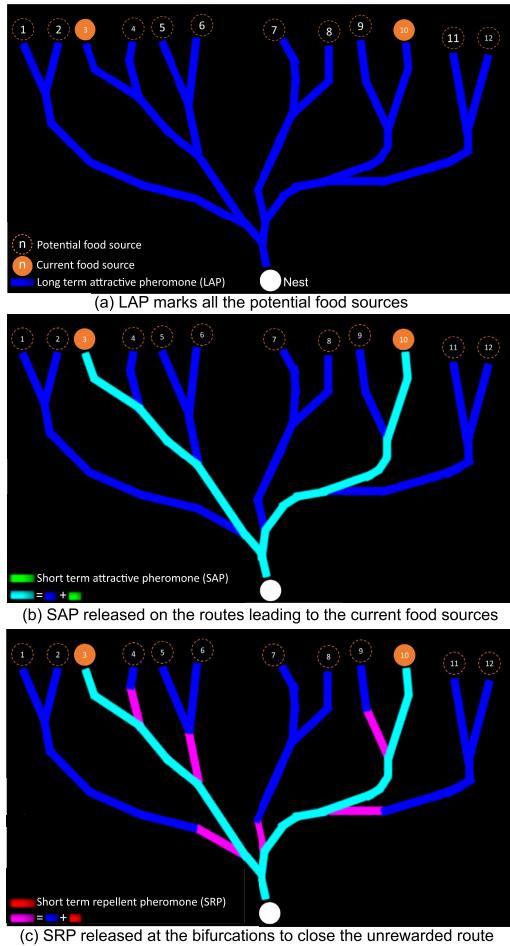
This case study is an example of pheromone trails following introduced in Section III-D3. Thus, the robot control strategy is mainly based on Algorithm. 1 but additionally incorporates three specifically defined pheromone types. To reach the correct food sites, a strategy, inspired by the behavior of real ants [7], has been devised such that the robots react to the different types of pheromones with prior probabilities shown in Fig. 13.

##### 3) RESULT

To evaluate the foraging performance, the successful rate ( $SR$ ) at which robot of each group successfully finds the current food sources is calculated by Eq.(13), where  $N$  is the number of trials and  $CF_i = 1$  if the robot has arrived at the current food source, otherwise  $CF_i = 0$ .

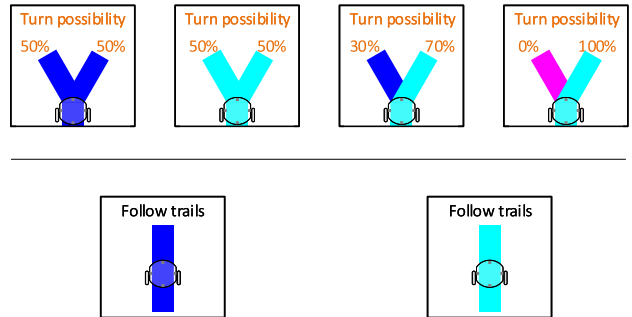
$$SR = \frac{1}{N} \sum_{i=0}^N CF_i \quad (13)$$

Fig. 14 shows the foraging performance of one robot in three groups with constant, available food sources 3 and 10.



**FIGURE 12.** Illustration of the settings of pheromone field for three groups of case study A: there are three basic kinds of pheromones, i.e., LAP (in blue), SAP (in green), SRP (in red), involved in the ant's foraging task. Note that the three pheromones can be selected for mixture in different representation (mixed pathway in cyan or magenta), but individually sensed by the robot. (a) For group 1 (G1 in the left-side text), LAP alone indicating foraging paths from the nest to the potential food sources, (b) For group 2 (G2), the pheromone pathway is mixed by two types of pheromone LAP and SAP, highlighting the currently available food source. (c) For group 3 (G3), the pheromone pathway is constructed by mixing three types of pheromones (LAP, SAP and SRP), further indicating the bifurcations from which a currently available food site cannot be found. Note that all these pheromone field settings mimic the real pheromone trail network in real ants.

The bar chart shows the frequency of arrival at each food point in  $N = 20$  trials for each group. The *SR* for G1 to G3 is 5%, 30% and 100%, showing clearly that making use of multiple pheromones significantly improves the food searching efficiency by successfully reaching the correct food sites. Note that the success rate in G2 is not satisfactory, this is caused by the probability setting as shown in Fig. 13. However, this success rate is line with the probabilistic analysis and significantly improved over G1. The arrival frequency distributions in Fig. 14 between the different groups help the understanding of multiple pheromones mechanism on improving food recruitment, and will hopefully encourage the



**FIGURE 13.** Robot control logic of Case study A: when facing bifurcations, the robot chooses the trail according to the turning possibility. In other cases, the robot follows the trails.

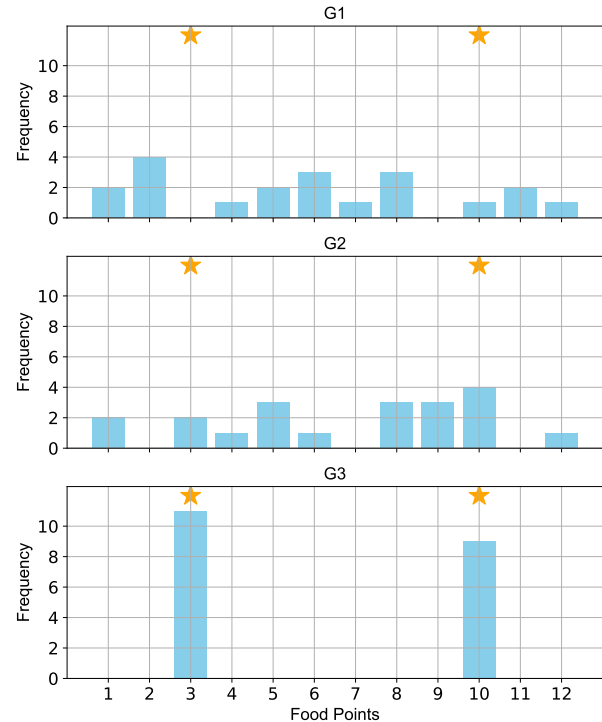


**FIGURE 14.** Arrival frequency distribution for each experimental group. The orange stars indicate the current available food source, which in this case are destinations 3 and 10. Note that sub-figures correspond to the pheromone maps depicted in Fig. 12.

use of multiple pheromone communication to address similar challenges in swarm robotics.

Moreover, Fig. 15, from the top-down facing camera of the localization system, depicts the trajectories of the robot in G3 based on the output from the localization system. The high overlap between the trajectories and the pheromone marked path in the background image again demonstrates the precision and accuracy of the localization system.

The experimental results of this case study have demonstrated the effective and flexible performance of the ColCOSΦ system, wherein different pheromones are correctly released to guide the robot to properly distinguish

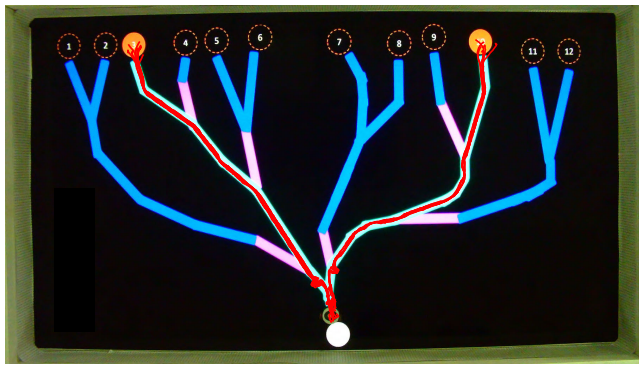


**FIGURE 15.** Trajectories of the foraging robot agent (20 trials) from experiments of group G3 of Case Study A. The background image is derived from a screen shot of the localization system video record.

between different types of pheromones corresponding to the successful simulation of ant's food recruitment task in reality.

### B. ATTRACTIVE OR REPULSIVE—HOW DO DIFFERENT PHEROMONES MODULATE SWARM BEHAVIOR?

In this case study, we explore how the multiple pheromones interact with each other and successively affect the agent's behavior in different tasks. To implement this, two tasks are devised by robots. The first task is to imitate the food carrying behavior of ants through the release of an aggregation type pheromone. The second task is to simulate the ability of one ant to warn other individuals of an incoming predator by releasing an alert type pheromone, so that they may escape from being captured. The second task thus is to test the roles of pheromones in protecting the swarm from incoming dangers.

#### 1) PHEROMONE FIELD CONSTRUCTION

The two types of pheromone are elucidated as follows:

- The aggregation pheromone (AGP) which is released by the leader robot for signaling the followers to gather together to simulate the food carrying behavior.
- The alarm pheromone (ALP) which is released by the robot in the vicinity of the predator to repel others from the site of danger.

The pheromone in this case study is modeled by Eq.(5). In this experiment, a quickly diffusing and evaporating pheromone is required, thus a short evaporation period is selected. Likewise, the diffusion factor is empirically selected to ensure an appropriate sensible distance-range for the robots.

The details of the parameter settings are listed in Table. 4. The injection of AGP is continuously updated according to the spontaneous position of the leader robot ( $\mathbf{P}_1$ ). The injection of ALP can be generated by any of follower robots ( $\mathbf{P}_j, j \in \{1, 2, 3, 4\}$ ) whose distance from the predator agent is less than a predetermined threshold.

**TABLE 4.** Pheromone parameter setting in case study B.

Type	Color	Model	Evaporation	Diffusion	Injection
AGP	Green	Eq.(5)	$e_\Phi = 10s$	$\sigma_x = 40cm$ $\sigma_y = 40cm$	$(\mu_x, \mu_y) = \mathbf{P}_1$
ALP	Red	Eq.(5)	$e_\Phi = 5s$	$\sigma_x = 60cm$ $\sigma_y = 60cm$	$(\mu_x, \mu_y) = \mathbf{P}_j, j \in \{1, 2, 3, 4\}$

#### 2) ROBOT CONTROL

This case study makes use of the gradient tracking and avoidance behavior introduced in Section III-D2. Hence the robot control strategy is based on the principles described in Section III-D2. Since, however, the goal of the three follower robots is to aggregate around the leader robot without being captured by the predator. We specifically designed control strategy for the leader robot and the follower robots, as illustrated in Algorithm 2 and Algorithm 3. As for the “predator” robot, it is permitted to wander freely in the arena without any special control.

#### Algorithm 2: The Control Strategy of the Leader

```

while robot power on do
  if no collision detected then
    if alarm pheromone detected then
      Calculate  $\theta_r$  of Alarm pheromone by Eq.(8);
      Move towards  $\theta_r$  direction by Eq.(14);
    else
      Wandering;
    else
      Collision avoidance;
  
```

#### Algorithm 3: The Control Strategy of Followers

```

while robot power on do
  if no collision detected then
    if alarm pheromone detected then
      Calculate  $\theta_r$  of alarm pheromone by Eq.(8);
      Move towards  $\theta_r$  direction by Eq.(14);
    else
      if aggregation pheromone detected then
        Calculate  $\theta_g$  of aggregation pheromone
        by Eq.(8);
        Move towards  $\theta_g$  direction by Eq.(14);
      else
        Wandering;
    else
      Collision avoidance;
  
```

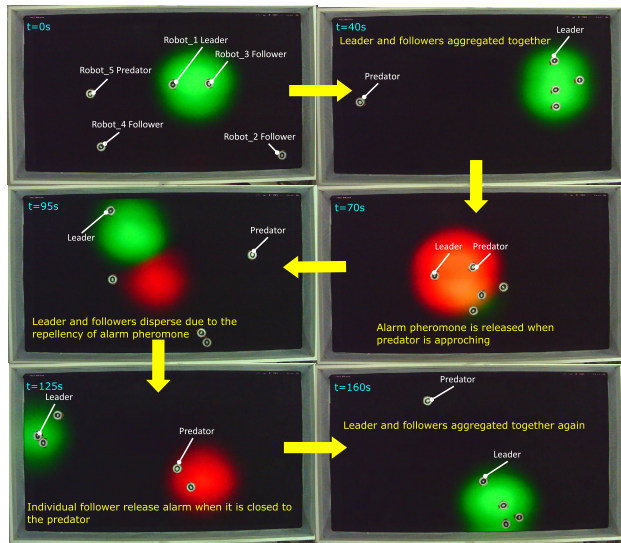


**FIGURE 16.** Snapshots of the screen taken during the execution case study B. The yellow arrows show the time-dependent order of the image.

Note that in this case study, we applied a bio-plausible approach called vector summation [42], [43] to integrate conflicting cues (e.g., attractive and repulsive pheromone, as shown in (10) and (11)). In this case study, how the output of vector summation is transformed to the speed of the robot motor is shown as follow:

$$\begin{cases} \omega_l = v_b - \alpha * (\theta_g - \theta_r) \\ \omega_r = v_b + \alpha * (\theta_g - \theta_r) \end{cases} \quad (14)$$

where:

- $\omega_l$  and  $\omega_r$  are the rotational speeds of left and right wheels respectively.
- $\theta_g$  and  $\theta_r$  are the positive gradient directions of the aggregation and alarm pheromones respectively, which can be calculated by Eq.(8).
- $\alpha$  is a sensitivity factor.
- $v_b$  is the base speed of the robot.

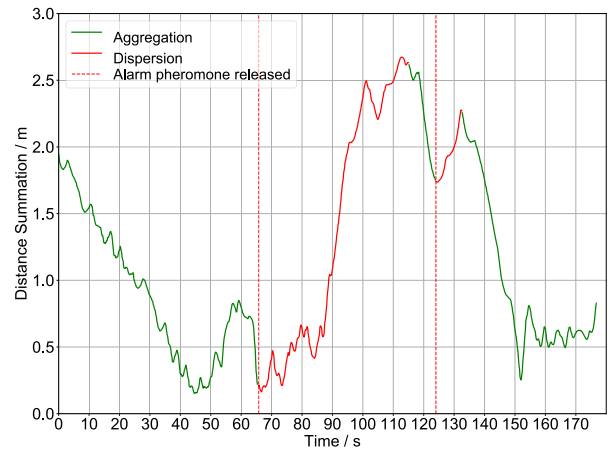
### 3) RESULT

Fig. 16 shows six snapshots captured by the top-down facing camera of the localization system during the experiment. These clearly demonstrate aggregation behavior stimulated by the presence of the attractive pheromone, and the dispersion behavior aroused by the repulsive pheromone.

In order to quantitatively evaluate how these two different pheromones affect the collective behaviors of swarm robots, we accumulate the Euclidean distances between the leader and the follower robots by Eq.(15) with respect to time:

$$S(t) = \sum_{i=2}^4 \sqrt{(x_i(t) - x_1(t))^2 + (y_i(t) - y_1(t))^2} \quad (15)$$

where  $i$  represents the robot ID,  $(x_i(t), y_i(t)) = \mathbf{P}_i(t)$  is the robot's position at time  $t$  and  $(x_1(t), y_1(t)) = \mathbf{P}_1(t)$



**FIGURE 17.** Summation of euclidean distances between every follower and the leader overtime. Different swarm robot behaviors are indicated by different colors. The time stamp is in line with Fig. 16.

is the leader's position at time  $t$ . The change of  $S(t)$  during one experiment is shown in Fig. 17, in which we can clearly see that the attractive pheromone evokes aggregation, thereby leading to a decrease in  $S$ , whilst the dispersion caused by the repulsive pheromone results in a dramatic increase in  $S$ .

The results of this case study have verified again the effectiveness and stability of our multiple pheromones system. During the experiment, the localization system can precisely track the spontaneous positions of all the robots, and the virtual pheromone can be released instantly on the screen and refreshed as required thereby guiding the behaviors of the swarm robots very timely.

### VI. DISCUSSION

It has become clear that the complexity and diversity of the information transmitted within a real insect colony is much higher than previously thought [45]. Part of this complex information involves the release and reaction to pheromones, which play essential roles in emerging collective behaviors in swarm robotics. The proposed ColCOSΦ artificial multiple pheromone system provides a unique facility in which to carry out in-depth studies in this area. By evaluating the performances of this system through preliminary experiments and two case studies, we have verified its capabilities and effectiveness.

The commonly observed, but poorly understood mechanisms by which multiple pheromones enable social insects to act collectively and thereby complete complex tasks was the underlying motivation to establish ColCOSΦ. We consider that this unique system will launch a new wave of research that will considerably enhance our understanding of pheromone-based communication. This will be highly relevant not only to elucidating the behavior of social insects, but also in the innovative development of swarm robotics, especially for the emergence of collective aggregation and foraging behaviors.

### A. ADDITIONAL PHEROMONE INSPIRED SCENARIOS

Building on the extensive studies into the trail pheromone of ants [28], [39], our system has enabled us to create a scenario in which different robotic agents will follow different leaders, demonstrating the potential to accomplish different tasks.

Inspired by the pheromone communication, research [46] proposed a pheromone-based method to find the shortest path between two points in a maze. This was followed later by the description of a “scent pervasion” based ant colony optimization (ACO) algorithm [47] to perform path planning within a complex environment like a maze. This “scent pervasion” mimics the diffusion of a chemical from its source to provide gradient information. These methods have all been tested using simulation methods rather than using real robots in a natural environment. However, we have now addressed this by implementing the model on our robot and testing it in our system. Thus, path planning may be solved by multiple pheromones.

Aggregation is another important, behavioral characteristic of swarm intelligence [48] and pheromone based aggregation has been recently demonstrated [49]. Similarly, other studies have used pheromones as communication tools to control robot distribution in an unknown environment [18], [50], [51]. All of these mechanisms can be investigated using our proposed system, where robots respond differently to different pheromones and finally form a specific distribution pattern.

It has been shown that colonies of *Leptothorax albipennis* ants make use of pheromones to estimate the size of a potential nest before emigrating from a destroyed nest [52]. This method, applied by the scouts (ant workers), can be hypothesized as the adaptation of the Buffon’s needle algorithm. Robotics studies have demonstrated the effectiveness of this approach [53] but with only a virtual robot. Using our new platform this model now can be implemented using a real robot.

### B. CHALLENGES

Several issues have emerged that require improvement. The visual tracking and localization system in this platform is crucial for releasing multiple pheromones. However, its current performance is challenged from two aspects: 1) A dim or uneven ambient light could affect the efficiency and accuracy of localization since a global on-demand threshold is used to search for the specific robot patterns; in its current form, a uniform-and-sufficient ambient light can guarantee expected performance. A promising solution to this problem is to apply a more adaptive or local threshold mechanism. 2) When the number of robot IDs exceeds 20, the difference in patterns becomes very small, which causes a decrease in the accuracy of ID recognition.

This work focuses on the early stages of swarm intelligence research, such as algorithm design, verification and optimization with real robots and sensory systems. At this stage, to the best of our knowledge, the proposed experimental

configuration is the optimal solution to emulate multiple pheromones, comparing to other similar works. Nevertheless, we are optimistic about the future that one algorithm can also go with real chemical substances. At that stage, the LCD and camera system may be no longer required. For example, in the application of ruins investigation and exploration, robot swarms can use different pheromones to mark hazard areas or high valuable areas to accelerate the exploration process.

### VII. CONCLUSION

In this paper, an effective, user-friendly and reliable multiple pheromones communication system named ColCOS $\Phi$  for swarm robotics research is proposed. The high-quality attributes of ColCOS $\Phi$  and the simplicity in implementing complex scenarios make the proposed system ready for complex swarm robots experiments. The research shown in this study has verified that complex collective behaviors can be generated via pheromone communications. The results from three case studies have demonstrated the potential of this system for swarm intelligence and swarm robotics study, particularly for collective behaviors such as foraging that rely on multiple pheromones communication.

### ACKNOWLEDGMENT

(Tian Liu and Xuelong Sun contributed equally to this work.)

### REFERENCES

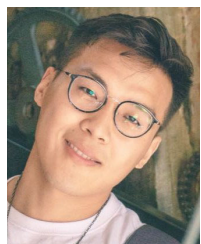
- [1] M. Brambilla, E. Ferrante, M. Birattari, and M. Dorigo, “Swarm robotics: A review from the swarm engineering perspective,” *Swarm Intell.*, vol. 7, no. 1, pp. 1–41, 2013.
- [2] N. Nedjah and L. S. Junior, “Review of methodologies and tasks in swarm robotics towards standardization,” *Swarm Evol. Comput.*, vol. 50, Nov. 2019, Art. no. 100565.
- [3] S. Camazine, J.-L. Deneubourg, N. R. Franks, J. Sneyd, E. Bonabeau, and G. Theraulaz, *Self-Organization in Biological Systems*, vol. 7. Princeton, NJ, USA: Princeton Univ. Press, 2003.
- [4] S. Garnier, J. Gautrais, and G. Theraulaz, “The biological principles of swarm intelligence,” *Swarm Intell.*, vol. 1, no. 1, pp. 3–31, 2007.
- [5] B. Hölldobler and E. O. Wilson, *The Ants*. Cambridge, MA, USA: Harvard Univ. Press, 1990.
- [6] G. E. Robinson, “Modulation of alarm pheromone perception in the honey bee: Evidence for division of labor based on hormonally regulated response thresholds,” *J. Comparative Physiol. A*, vol. 160, no. 5, pp. 613–619, 1987.
- [7] E. J. Robinson, D. E. Jackson, M. Holcombe, and F. L. Ratnieks, “Insect communication: ‘no entry’ signal in ant foraging,” *Nature*, vol. 438, no. 7067, p. 442, 2005.
- [8] E. J. H. Robinson, K. E. Green, E. A. Jenner, M. Holcombe, and F. L. W. Ratnieks, “Decay rates of attractive and repellent pheromones in an ant foraging trail network,” *Insectes Sociaux*, vol. 55, no. 3, pp. 246–251, Sep. 2008.
- [9] K. M. Salama, A. M. Abdelbar, F. E. B. Otero, and A. A. Freitas, “Utilizing multiple pheromones in an ant-based algorithm for continuous-attribute classification rule discovery,” *Appl. Soft Comput.*, vol. 13, no. 1, pp. 667–675, 2013.
- [10] K. Ye, C. Zhang, J. Ning, and X. Liu, “Ant-colony algorithm with a strengthened negative-feedback mechanism for constraint-satisfaction problems,” *Inf. Sci.*, vols. 406–407, pp. 29–41, Sep. 2017.
- [11] A. H. Purnamadjaja and R. A. Russell, “Guiding robots’ behaviors using pheromone communication,” *Auto. Robots*, vol. 23, no. 2, pp. 113–130, Aug. 2007.
- [12] O. Simonin, T. Huriaux, and F. Charpillet, “Interactive surface for bio-inspired robotics, re-examining foraging models,” in *Proc. IEEE 23rd Int. Conf. Tools With Artif. Intell.*, Nov. 2011, pp. 361–368.

- [13] S. Okdem and D. Karaboga, "Routing in wireless sensor networks using an ant colony optimization (ACO) router chip," *Sensors*, vol. 9, no. 2, pp. 909–921, Feb. 2009.
- [14] G.-Z. Yang, J. Bellingham, P. E. Dupont, P. Fischer, L. Floridi, R. Full, N. Jacobstein, V. Kumar, M. McNutt, R. Merrifield, B. J. Nelson, B. Scassellati, M. Taddeo, R. Taylor, M. Veloso, Z. L. Wang, and R. Wood, "The grand challenges of science robotics," *Sci. Robot.*, vol. 3, no. 14, Jan. 2018, Art. no. eaar7650.
- [15] M. Dorigo, G. Theraulaz, and V. Trianni, "Swarm robotics: Past, present, and future," *Proc. IEEE*, vol. 109, no. 7, pp. 1152–1165, Jul. 2021.
- [16] T. Schmickl, R. Thenius, C. Moeslinger, G. Radspieler, S. Kernbach, M. Szymanski, and K. Crailsheim, "Get in touch: Cooperative decision making based on robot-to-robot collisions," *Auto. Agents Multi-Agent Syst.*, vol. 18, no. 1, pp. 133–155, Feb. 2009.
- [17] N. R. Hoff, A. Sagoff, R. J. Wood, and R. Nagpal, "Two foraging algorithms for robot swarms using only local communication," in *Proc. IEEE Int. Conf. Robot. Biomimetics*, Dec. 2010, pp. 123–130.
- [18] D. Payton, M. Daily, R. Estowski, M. Howard, and C. Lee, "Pheromone robotics," *Auto. Robots*, vol. 11, no. 3, pp. 319–324, 2001.
- [19] T. Liu, X. Sun, C. Hu, Q. Fu, H. Isakhani, and S. Yue, "Investigating multiple pheromones in swarm robots—A case study of multi-robot deployment," in *Proc. 5th Int. Conf. Adv. Robot. Mechatronics (ICARM)*, Dec. 2020, pp. 595–601.
- [20] J. L. Farrugia and S. G. Fabri, "Swarm robotics for object transportation," in *Proc. UKACC 12th Int. Conf. Control (CONTROL)*, Sep. 2018, pp. 353–358.
- [21] L. Paull, J. Tani, H. Ahn, J. Alonso-Mora, L. Carlone, M. Cap, Y. F. Chen, C. Choi, J. Dusek, Y. Fang, and D. Hoehener, "Duckietown: An open, inexpensive and flexible platform for autonomy education and research," in *Proc. IEEE Int. Conf. Robot. Autom. (ICRA)*, May 2017, pp. 1497–1504.
- [22] A. Vitanza, P. Rossetti, F. Mondada, and V. Trianni, "Robot swarms as an educational tool: The Thymio's way," *Int. J. Adv. Robotic Syst.*, vol. 16, no. 1, Jan. 2019, Art. no. 172988141882518.
- [23] R. T. Cardé and A. K. Minks, *Insect Pheromone Research: New Directions*. Boston, MA, USA: Springer, 2012.
- [24] N. Vaughan, "Swarm communication by evolutionary algorithms," in *Proc. IEEE Conf. Evolving Adapt. Intell. Syst. (E AIS)*, May 2018, pp. 1–9.
- [25] A. Reina, A. J. Cope, E. Nikolaidis, J. A. R. Marshall, and C. Sabo, "ARK: Augmented reality for kilobots," *IEEE Robot. Autom. Lett.*, vol. 2, no. 3, pp. 1755–1761, Jul. 2017.
- [26] M. Mamei and F. Zambonelli, "Physical deployment of digital pheromones through RFID technology," in *Proc. IEEE Swarm Intell. Symp. (SIS)*, Jun. 2005, pp. 281–288.
- [27] R. A. Russell, "Heat trails as short-lived navigational markers for mobile robots," in *Proc. Int. Conf. Robot. Autom.*, vol. 4, Apr. 1997, pp. 3534–3539.
- [28] K. Sugawara, T. Kazama, and T. Watanabe, "Foraging behavior of interacting robots with virtual pheromone," in *Proc. IEEE/RSJ Int. Conf. Intell. Robots Syst. (IROS)*, Oct. 2004, pp. 3074–3079.
- [29] N. Kitamura, Y. Nakamichi, and K. Fukuda, "Development of a desktop swarm robot system based on pheromone communication," *Artif. Life Robot.*, vol. 14, no. 3, p. 329, 2009.
- [30] R. Mayet, J. Roberz, T. Schmickl, and K. Crailsheim, "Antbots: A feasible visual emulation of pheromone trails for swarm robots," in *Proc. Int. Conf. Swarm Intell.* Berlin, Germany: Springer, 2010, pp. 84–94.
- [31] M. Salman, D. Garzón Ramos, K. Hasselmann, and M. Birattari, "Phormica: Photochromic pheromone release and detection system for stigmergy coordination in robot swarms," *Frontiers Robot. AI*, vol. 7, p. 195, Dec. 2020.
- [32] F. Arvin, T. Krajnik, A. E. Turgut, and S. Yue, "COS $\phi$ : Artificial pheromone system for robotic swarms research," in *Proc. IEEE/RSJ Int. Conf. Intell. Robots Syst. (IROS)*, Sep. 2015, pp. 407–412.
- [33] X. Sun, T. Liu, C. Hu, Q. Fu, and S. Yue, "ColCOS  $\phi$ : A multiple pheromone communication system for swarm robotics and social insects research," in *Proc. IEEE 4th Int. Conf. Adv. Robot. Mechatronics (ICARM)*, Jul. 2019, pp. 59–66.
- [34] S. Na, Y. Qiu, A. E. Turgut, J. Ulrich, T. Krajnik, S. Yue, B. Lennox, and F. Arvin, "Bio-inspired artificial pheromone system for swarm robotics applications," *Adapt. Behav.*, vol. 29, no. 4, pp. 395–415, Aug. 2021.
- [35] G. Valentini, A. Antoun, M. Trabattoni, B. Wiandt, Y. Tamura, E. Hocquard, V. Trianni, and M. Dorigo, "Kilogrid: A novel experimental environment for the Kilobot robot," *Swarm Intell.*, vol. 12, no. 3, pp. 245–266, Sep. 2018.
- [36] I. Susnea, G. Vasiliu, A. Filipescu, and A. Radaschin, "Virtual pheromones for real-time control of autonomous mobile robots," *Stud. Inform. Control*, vol. 18, no. 3, pp. 233–240, 2009.
- [37] T. Sakakibara and D. Kurabayashi, "Artificial pheromone system using RFID for navigation of autonomous robots," *J. Bionic Eng.*, vol. 4, no. 4, pp. 245–253, Dec. 2007.
- [38] A. A. Khaliq and A. Saffiotti, "Stigmergy at work: Planning and navigation for a service robot on an RFID floor," in *Proc. IEEE Int. Conf. Robot. Autom. (ICRA)*, May 2015, pp. 1085–1092.
- [39] R. Fujisawa, H. Imamura, and F. Matsuno, "Cooperative transportation by swarm robots using pheromone communication," in *Distributed Autonomous Robotic Systems*. Berlin, Germany: Springer, 2013, pp. 559–570.
- [40] T. Krajník, M. Nitsche, J. Faigl, P. Vaněk, M. Šaska, L. Přeučil, T. Duckett, and M. Mejail, "A practical multirobot localization system," *J. Intell. Robotic Syst.*, vol. 76, nos. 3–4, pp. 539–562, Dec. 2014.
- [41] C. Hu, Q. Fu, and S. Yue, "Colias IV: The affordable micro robot platform with bio-inspired vision," in *Proc. Annu. Conf. Towards Auto. Robotic Syst.* Cham, Switzerland: Springer, 2018, pp. 197–208.
- [42] X. Sun, M. Mangan, and S. Yue, "An analysis of a ring attractor model for cue integration," in *Proc. Conf. Biomimetic Biohybrid Syst.* Cham, Switzerland: Springer, 2018, pp. 459–470.
- [43] T. Hoinvile and R. Wehner, "Optimal multiguidance integration in insect navigation," *Proc. Nat. Acad. Sci. USA*, vol. 115, no. 11, pp. 2824–2829, Mar. 2018.
- [44] D. E. Jackson and F. L. W. Ratnieks, "Communication in ants," *Current Biol.*, vol. 16, no. 15, pp. R570–R574, Aug. 2006.
- [45] S. D. Leonhardt, F. Menzel, V. Nehring, and T. Schmitt, "Ecology and evolution of communication in social insects," *Cell*, vol. 164, no. 6, pp. 1277–1287, Mar. 2016.
- [46] M. Szymanski, T. Breitling, J. Seyfried, and H. Wörn, "Distributed shortest-path finding by a micro-robot swarm," in *Proc. Int. Workshop Ant Colony Optim. Swarm Intell.* Berlin, Germany: Springer, 2006, pp. 404–411.
- [47] X. Chen, Y. Kong, X. Fang, and Q. Wu, "A fast two-stage ACO algorithm for robotic path planning," *Neural Comput. Appl.*, vol. 22, no. 2, pp. 313–319, Feb. 2013.
- [48] L. Bayindir, "A review of swarm robotics tasks," *Neurocomputing*, vol. 172, pp. 292–321, Jan. 2016.
- [49] F. Arvin, A. E. Turgut, T. Krajnik, S. Rahimi, I. E. Okay, S. Yue, S. Watson, and B. Lennox, " $\Phi$  clust: Pheromone-based aggregation for robotic swarms," in *Proc. IEEE/RSJ Int. Conf. Intell. Robots Syst. (IROS)*, Oct. 2018, pp. 4288–4294.
- [50] J. L. Pearce, B. Powers, C. Hess, P. E. Rybski, S. A. Stoeter, and N. Papanikopoulos, "Using virtual pheromones and cameras for dispersing a team of multiple miniature robots," *J. Intell. Robotic Syst.*, vol. 45, no. 4, pp. 307–321, Apr. 2006.
- [51] G. Silva, J. Costa, T. Magalhães, and L. P. Reis, "Cyberrescue: A pheromone approach to multi-agent rescue simulations," in *Proc. 5th Iberian Conf. Inf. Syst. Technol.*, Jun. 2010, pp. 1–6.
- [52] E. B. Mallon and N. R. Franks, "Ants estimate area using Buffon's needle," *Proc. Roy. Soc. London. Ser. B, Biol. Sci.*, vol. 267, no. 1445, pp. 765–770, Apr. 2000.
- [53] E. Sahin and N. R. Franks, "Measurement of space: From ants to robots," in *Proc. WGW EPSRC/BBSRC Int. Workshop Biologically-Inspired Robot. Legacy W. Grey Walter*. Princeton, NJ, USA: Citeseer, 2002, pp. 241–247.



**TIAN LIU** received the B.Eng. degree from Chongqing University, Chongqing, China, in 2016. He is currently pursuing the Ph.D. degree with the University of Lincoln, Lincoln, U.K.

In 2018, he visited the Machine Life and Intelligence Research Center, Guangzhou University, Guangzhou, China. His research interests include swarm intelligence, swarm robotics, microrobot, and bio-inspired algorithms, especially by pheromone. He was awarded the Marie Curie Fellowship to be involved in EU FP7 projects HAZCEPT (318907), the EU Horizon 2020 projects STEP2DYNA (691154), and ULTRACEPT (778062) as a Research Assistant.



**XUELONG SUN** received the B.Eng. degree from Chongqing University, Chongqing, China, in 2016, and the Ph.D. degree in computer science from the University of Lincoln, Lincoln, U.K., in 2021.

He was awarded the Marie Curie Fellowship to be involved in the EU Horizon 2020 projects STEP2DYNA (691154) as a Research Assistant with Tsinghua University, from June 2017 to June 2018, and ULTRACEPT (778062) as a Research Assistant with Guangzhou University, from January 2019 to March 2019, and from November 2019 to May 2020. He is mainly studying the modeling of insect navigation, including visual navigation and path integration. His research interests include the pheromone-based swarm intelligence of social insects and investigating the potential applications in robotics.



**QINBING FU** (Member, IEEE) received the B.Sc. degree from the University of Electronic Science and Technology of China, in 2009, and the M.Sc. degree (by Research) and the Ph.D. degree from the University of Lincoln, in 2014 and 2018, respectively.

He is currently a Lecturer with the School of Mathematics and Information Science, Guangzhou University. He is also works with the Machine Life and Intelligence Research Centre, Guangzhou University. He is an Honorary Research Fellow with the School of Computer Science, University of Lincoln. He was awarded the Marie Curie Fellowship to be involved in the EU FP7 projects EYE2E (269118) and LIVCODE (295151), EU Horizon 2020 projects STEP2DYNA (691154) and ULTRACEPT (778062) as a Research Assistant with the School of Mathematics and Statistics, Xi'an Jiaotong University, Xi'an, China, and the Institute of Microelectronics, Tsinghua University, Beijing, China, from 2014 to 2018. His current research interests include brain-inspired intelligence, motion vision, neural networks, robotics, and machine learning. He is a member of the International Neural Network Society (INNS) and the International Society for Artificial Life (ISAL).



**CHENG HU** (Member, IEEE) received the B.Eng. degree from the College of Opt-Electronics Engineering, Chongqing University, Chongqing, China, in 2013, and the Ph.D. degree from the University of Lincoln, Lincoln, U.K., in 2018.

In 2014, he visited the Institute of Microelectronics, Tsinghua University, Beijing, China, as a Research Assistant. In 2014, he visited the Institute of Rehabilitation and Medical Robotics, Huazhong University of Science and Technology, Wuhan, China. He is currently a Lecturer and an Administrator with the Machine Life and Intelligence Research Center, Guangzhou University, and an Honorary Postdoctoral Research Fellow at the University of Lincoln. His current research interests include bio-inspired algorithms, bio-robotics, visual sensors, and signal processing. He was a recipient of the Marie Curie Fellowship to be involved in the EU FP7 projects EYE2E (269118) and LIVCODE (295151) and EU Horizon 2020 projects STEP2DYNA (691154) and ULTRACEPT (778062).



**SHIGANG YUE** (Senior Member, IEEE) received the M.Sc. and Ph.D. degrees from the Beijing University of Technology (BJUT), Beijing, China, in 1993 and 1996, respectively.

He was with BJUT as a Lecturer, from 1996 to 1998, and an Associate Professor, from 1998 to 1999. He was an Alexander von Humboldt Research Fellow with the University of Kaiserslautern, Kaiserslautern, Germany, from 2000 to 2001. He held research positions at the University of Cambridge, Cambridge, U.K.; Newcastle University, Newcastle upon Tyne, U.K.; and the University College London (UCL), London, U.K.; from 2002 to 2007. In 2007, he joined the University of Lincoln, Lincoln, U.K., as a Senior Lecturer. He was promoted to a Professor, in 2012, where he is currently a Professor (part-time) with the School of Computer Science. He also holds a Professorship with the Machine Life and Intelligence Research Centre, Guangzhou University, Guangzhou, China, in collaboration with Prof. J. Peng. His current research interests include artificial intelligence, computer vision, robotics, intelligent transportation, brains, and neuroscience.

Dr. Yue is a member of the International Neural Network Society (INNS) and the International Society of Bionic Engineering (ISBE).